# Stochastic Optimization of Sub-Hourly Economic Dispatch With Wind Energy

Harsha Gangammanavar, Suvrajeet Sen, and Victor M. Zavala

***Abstract*—We present a stochastic programming framework for a multiple timescale economic dispatch problem to address integration of renewable energy resources into power systems. This framework allows certain slow-response energy resources to be controlled at an hourly timescale, while fast-response resources, including renewable resources, and related network decisions can be controlled at a sub-hourly timescale. To this end, we study two models motivated by actual scheduling practices of system operators. Using an external simulator as driver for sub-hourly wind generation, we optimize these economic dispatch models using stochastic decomposition, a sample-based approach for stochastic programming. Computational experiments, conducted on the IEEE-RTS96 system and the Illinois system, reveal that optimization with sub-hourly dispatch not only results in lower expected operational costs, but also predicts these costs with far greater accuracy than with models allowing only hourly dispatch. Our results also demonstrate that when compared with standard approaches using the extensive formulation of stochastic programming, the sequential sampling approach of stochastic decomposition provides better predictions with much less computational time.**

***Index Terms*—Economic dispatch, stochastic decomposition, sub-hourly dispatch.**

## I. Introduction

THE integration of renewable resources into energy networks, especially in large scale power grids, poses several technological and operational challenges. Among renewable resources, wind and solar energy fall under the class of variable/intermittent energy resources because of their inherent stochasticity. Their variability is not only high in magnitude, but they also exhibit sub-hourly fluctuations. In addition, these resources are known to have a temporal mismatch with the load. These characteristics have generated significant academic interest as well as several new initiatives by power system operators to harness the full benefits of renewable resources.

Manuscript received June 10, 2014; revised October 16, 2014, December 09, 2014, and January 15, 2015; accepted February 17, 2015. Date of publication March 23, 2015; date of current version February 17, 2016. The work of V. M. Zavala was supported by the U.S. Department of Energy, Office of Science, under contract number DE-AC02-06CH11357. This work was supported by NSF (CMMI: 0900070) and AFOSR (FA9550–13-1–0015). Paper no. TPWRS-00790-2014.

H. Gangammanavar and S. Sen are with the Daniel J. Epstein Department of Industrial and Systems Engineering, University of Southern California, Los Angeles, CA 90089 USA (e-mail: gangamma@usc.edu; s.sen@usc.edu).

V. M. Zavala is with the Mathematics and Computer Science Division, Argonne National Laboratory, Argonne, IL 60439 USA (e-mail: vzavala@mcs.anl.gov).

Color versions of one or more of the figures in this paper are available online at http://ieeexplore.ieee.org.

Digital Object Identifier 10.1109/TPWRS.2015.2410301

Renewable integration challenges also necessitate incorporation of faster reserves, storage devices and similar services operating alongside the slow ramping conventional generators in the energy network. To maintain robustness of such a network, their operations should be planned by appropriately modeling the decision processes and using solution approaches that provide verifiable performance.

Currently, power systems planning is mostly based on a two level hierarchy: day-ahead unit commitment (DAUC) and economic dispatch (ED). A substantial number of studies ([1]–[3]) have focused on DAUC in the presence of renewable energy resources. By definition, the DAUC models use a 24-h horizon with 1-h resolution and set the initial commitment status for all generation units. Operating reserves and other regulation capacities are also procured in the day-ahead market [4], [5]. Some power system operators also use short-term unit commitment and real-time unit commitment to update the initial commitments based on new load and renewable generation forecasts, and schedule additional operating reserves. Once the commitments are set and the reserves requirements are established, dispatch schedules (generator set points) are determined by solving the ED model which is the focus of our work.

Due to grid characteristics, the operating practices vary significantly across balancing authorities. For example, the generation scheduling process in Bonneville Power Administration (BPA), a U.S. government electric utility in the Pacific Northwest, is based on hourly bulk energy schedules [6]. BPA can control hydro-generation within an hour, but is unable to access thermal generation within its balancing authority area on a sub-hourly basis. The economic dispatch of conventional generation is based on an hour-ahead forecast and is completed 20 min before the hour of delivery. BPA normally has sufficient range of load-following, regulation, and ramping capabilities to handle within-hour imbalances. Advanced ISOs, CAISO for example, use an hour-ahead scheduling process (HASP) and a real-time dispatch (RTD) optimization to handle short term energy imbalances. The RTD process runs every 5 min with a horizon of 65 min to dispatch internal resources [6]. The intertie resources however, are scheduled non-dynamically for an hour by HASP. Similar operating practices, where certain resources are scheduled at a coarse timescale and others are scheduled at a fine timescale, are used in European TSOs and other balancing authorities in North America. Moreover, deterministic optimization models based on a single scenario are used in this process.

Worldwide, electricity grids are in transition, and recently there are proposals which suggest several reforms to current practices to enable better integration of variable generation (e.g.,

FERC Order-764 in the U.S. [7]). They require variable generator owners to provide sub-hourly generation and outage data, and power system operators to use sub-hourly scheduling for all generation resources. Balancing authority area operators and ISOs are at different stages to accommodate these changes. For example, within-hour scheduling at 10-min intervals is being considered for implementation at BPA [6]. Moreover, the need for advanced optimization tools and simulation softwares has been identified as a major requirement for efficient implementation of sub-hourly dispatch [8].

In this regard, there have been simulation based investigations of sub-hourly dispatch. For example, the CAISO 2010 report ([9], Appendix C) reveals that sub-hourly analysis tends to overcome relatively small operational issues identified by hourly simulations. However, if the hourly simulations indicate more significant issues, then the sub-hourly simulation shows even larger impact. In another recent work [10], the authors study a power system with renewable resources using a simulation based framework, which integrates system operations at multiple timescales. The authors study the impact of renewable generation variability at different sub-hourly time resolutions and the impact of uncertainty by using different forecasts. Their study shows higher energy imbalance and greater transmission congestion with hourly time resolution, compared to sub-hourly resolutions. Unfortunately, most optimization studies which are based on average processes (e.g., hourly resolution models) tend to choose "optimal" settings with little room for error [11]. Based on the operational issues identified in [9] and [10], one can draw similar conclusions for hourly simulation based unit commitment and economic dispatch models. In our study we incorporate optimization as well as simulation at hourly and sub-hourly timescales respectively.

Sub-hourly dispatch has been used for ED in the short-term unit commitment model of [12]. The authors consider 10-min resolution for dispatch and compute the commitments using only 10 scenarios. These studies ([1]–[5]) usually employ approximations which reduce the original model formulation (with a larger set of scenarios) to a much smaller, and computationally manageable model [13]. While such a strategy tends to achieve tractability in optimization, the quality of predictions from such models can be suspect. In Section III (discussions related to Tables I and II) we will highlight issues resulting from both small sample approximations as well as hourly wind aggregation in the context of large scale economic dispatch.

To better harvest the benefits of renewable integration one needs to address the following important questions:

- What is the impact of increased variability from renewable generation on economic dispatch? Many jurisdictions in U.S. are mandating significant increases in renewable generation. Such mandates have the potential of introducing far more variability in the electricity generation than has ever been experienced.
- What optimization tools should be used to make choices that will mitigate the impact of increased variability?
- How similar are the decisions obtained from models which have different update intervals for variable generation? More frequent updates demand greater investments in resources for computations and operations. Depending on how similar these decisions are, a system operator has the option to choose computational resources in a cost effective manner.

With the above questions in mind, the main contributions of this work are:

- A stochastic decomposition (2-SD, [14]) framework which can accommodate system operations at multiple timescales as well as exogenous information from state-of-the-art forecast simulators. This framework allows us to plan dispatch operations more effectively than deterministic and/or coarse grained hourly models by making decisions based on a large set of future possibilities. Moreover, the 2-SD framework derives its scalability from its decomposition-based sequential sampling framework which identifies the sample size during the algorithmic process. This is particularly relevant because of sub-hourly wind variability. This algorithmic approach is presented in Section II.
- Our computational results are the first of its kind, showing that a) 2-SD provides a viable computational framework for realistic economic dispatch models in the presence of hourly and sub-hourly resource allocation, and b) finer resolution models of wind lead to somewhat higher generation from slow ramping generators to enhance the reliability (i.e., reduce dependence on high cost reserves). These results are presented in Section III.

## II. Economic Dispatch Under Uncertainty

Stochastic programming (SP) has been widely used for power systems applications such as stochastic unit commitment, establishing reserve requirements, and others. Benders decomposition is used in [1] and [12] with a master unit commitment problem, and subproblems to check feasibility of the master solution. In [15], a Lagrangian relaxation algorithm is employed in which a first stage problem schedules slow generators, and a second stage subproblem is used for committing fast generators and dispatch all resources. In [16], robust optimization, with the objective to minimize the worst-case cost associated with commitment solutions, is used in conjunction with stochastic optimization within a unified Benders framework. In [17], the unit commitment horizon is divided into two parts. While stochastic optimization is used for the first part, the second part is solved using interval unit commitment by considering only the central forecast, an upper bound and a lower bound on uncertainty. In all these studies a representative set (with size 10–100) of scenarios is used for optimization. Increasing the number of scenarios often result in very large models, and requires parallelization over a large cluster of computers for optimization [2]. To the best of our knowledge, our work provides the first real scale application of SP to the economic dispatch problem. In order to relate the economic dispatch problem to SP, we first present a general framework. Following this setup we will identify two alternative operating practices, one motivated by the time lines of BPA and the other by advanced ISOs like CAISO [6].

### A. General Framework

We use a two-stage stochastic linear programming framework in which we distinguish between decisions $(x)$ which are made prior to the observation of a random event, and decisions $(y)$

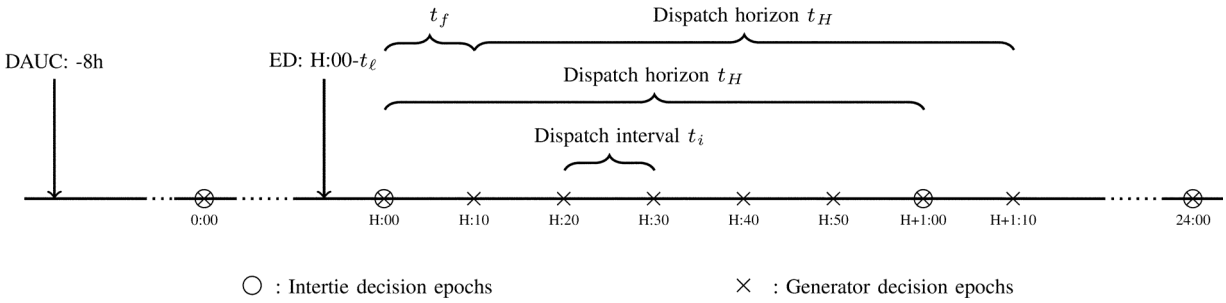


Fig. 1. Dispatch scheduling process with $t_f = 10$ min.

which respond adaptively to the initial choice $(x)$ and the observation $(\omega)$. In the SP literature these adaptive decisions are referred to as recourse decisions. The representation of *two-stage stochastic linear program with recourse* (2SLP) is given by

$$\min_{x\in\Re^{n_1}} f(x) := c^\top x + \mathbb{E}\{h(x,\tilde{\omega})\} \quad s.t. Ax \le b \tag{1a}$$

where

$$h(x,\omega) = \min_{y\in\Re^{n_2}} d^\top y \quad s.t. Wy = r(\omega) - Tx \quad y \ge 0. \tag{1b}$$

Here, $\omega$ is a realization of the random variable $\tilde{\omega}$. The SP literature refers to (1a) as the first stage and (1b) as the second stage.

Ordinarily, the number of possible future scenarios can be so large that the expectation in (1) can only be approximated by either a) scenario sampling, or b) selecting a small subset of scenarios [18]. In either case, we obtain a prediction of the cost associated with decisions realized from a model. It is customary to verify the quality of these predictions using large sample Monte Carlo simulations.

When the probability space is limited to a finite number $(S)$ of scenarios, the problem can be reformulated as one large deterministic problem:

$$\begin{aligned} &\min c^\top x + \sum_{s=1}^{S} p^s (d^\top y^s) \\ &s.t. Ax \le b \\ &Wy^s = r(\omega^s) - Tx \quad s = 1,\ldots,S \\ &y^s \ge 0 \quad s = 1,\ldots,S. \end{aligned} \tag{2}$$

Here $p^s$ denotes the probability of scenario $s$. For methods using Monte Carlo simulation, the number of scenarios is chosen based on computing resources (the platform and the solver) available, and for such instances one uses $p^s = 1/S$. We will refer to this formulation (2) as the *extensive scenario formulation* (ESF). A very special case of ESF, using a single forecast scenario, is the deterministic dispatch model commonly employed by power system operators. In the following we summarize the time lines and practices as they exist today.

### *B. Scheduling Time Lines and Practices*

The scheduling process for hour $H$ begins at $H - t_\ell$ (Fig. 1), where the leadtime $t_\ell$ varies from 7.5 min (at CAISO) to 20 min (at BPA). We assume that the generators are already committed by solving the unit commitment problem (and started) so that sufficient resources are available to supply the expected load. We also assume that the fast-start generators and other load following reserves, as well as regulating reserves have been procured to accommodate fine grain fluctuations. These unit commitments and reserve levels, along with current generation levels, are used as input to our dispatch models. At time $H - t_\ell$, the renewable generation and demand forecasts are locked down and are used to build the model. The dispatch model uses a horizon $t_H$ of about an hour which includes fine grain time intervals at which the variable generation information is updated. This time interval is denoted $t_i$ and typically ranges from 10 min to 60 min. This process is run every $t_f$ min throughout the day, when the generation set points can be revised.

We will study two alternative practices depending on the interval of time between updates of slow-response conventional generation:

1) *Hourly coupling models* only allow hourly updates of slow-response generators and reflect the scheduling practices at some balancing authority areas, e.g., BPA [6]. In this model the slow-response generators and intertie resource decisions constitute the first stage decision variable $x$. Both these decisions are updated every hour, that is $t_f = 60$ min. The fast-response reserves, intermittent resources, and network decisions are controlled in an adaptive manner at fine timescale every $t_i$ min. Note that fast-response reserves refer to those generators and load following reserves which have response times much lower than 10 min (the finest resolution considered) [19]. In addition, the second stage will accommodate the revised slow-response conventional generation decisions for the next hour. Since the slow-response generators are fixed for the hour, intra-hour energy imbalance is completely handled through fast-response reserves. All these fine grain decisions are lumped together in our second stage variable $y$.
2) *Sub-hourly coupling models*, on the other hand, allow slow-response generator decisions to be updated at sub-hourly intervals. These models are motivated by system operations at advanced ISOs like CAISO [6]. For dispatch beginning at the hour (i.e., time H) one uses the

slow-response generators and intertie resource decisions as first stage decision variable $x$. The generator decisions are fixed only for $t_f = 10$ min, at which point in time, these decisions can be revised. On the other hand, the intertie decisions are fixed for the hour. For dispatch starting at intra-hour epochs (time $H + nt_f$, $n = 1, 2, \ldots$), only slow-response generator decisions constitute the first stage variable $x$. Revisions at future sub-hourly time periods and next hour intertie decisions, which fall within the model horizon $t_H$, are included as second stage variables. These, along with fast-response reserves, intermittent resources and network decisions constitute the variable $y$. Since sub-hourly revisions are considered in this model, hourly coupling decisions are excluded.

### C. Alternative Aggregations in Dispatch Models

As mentioned earlier, studies based on pure hourly dispatch models have the potential to hide the complications arising from sub-hourly variability of intermittent resources. To investigate the impact of sub-hourly decisions in the presence of other hourly decisions, we compare dispatch models at different sub-hourly resolutions. The second stage in the 2-SLP model (1a)–(1b) at the finest resolution (10 min) includes linear constraints for each sub-hourly interval-$n$: $\{\mathcal{F}(x, y_n, r(\omega_n)) = 0, y_n \geq 0\}$ for $n = 1, \ldots, 6$. This considerably increases the size of the problem, but identifies the value of fine grain information in deciding the slow-response conventional generation and intertie levels.

The *aggregated models* at 20-, 30-, and 60-min resolutions, on the other hand, are created by aggregating the constraints and variables of (1b) by an averaging process. For example, to create the aggregated hourly model we define $\bar{y} = 1/6 \sum_{n=1}^{6} y_n$, and the quantity $r(\omega_n)$ is replaced by the observed average $1/6 \sum_{n=1}^{6} r(\omega_n)$. In this case, we therefore rewrite the sub-hourly constraints as $\mathcal{F}(x, \bar{y}, 1/6 \sum_{n=1}^{6} r(\omega_n)) = 0$. Clearly, these models are aggregations of the 10-min model. Nevertheless, these are different instantiations of two-stage stochastic programming models. It is worthwhile to note that the 60-min aggregated model reflects current operations at BPA, where conventional decisions are revised once every hour based on hourly bulk variable generation information.

### D. Algorithms for the Study

All dispatch models were formulated in the 2SLP and ESF forms. As long as the scenarios can be enumerated easily the ESF formulation (2) can be solved as one large LP using state-of-the-art deterministic solvers like CPLEX. Alternatively, one could use some deterministic decomposition scheme for ESF such as Benders' decomposition, Dantzig-Wolfe decomposition or the progressive hedging algorithm [3]. In this paper, the 2SLP problem (1) is solved using two-stage stochastic decomposition algorithm (2-SD) [14].

Conceptually, 2-SD is a stochastic version of deterministic Benders' decomposition [20] or L-shaped method [21]. Like these decomposition methods, 2-SD constructs a piecewise linear approximation to the recourse function and updates the approximation during each iteration of the algorithm. But unlike the deterministic methods, the recourse function is estimated for a small number of outcomes $\omega$ of random variable $\tilde{\omega}$. Moreover, because of its sampling based approximations, it is not restricted to only those instances in which the random variables are discrete. This allows 2-SD to be used with external simulators. This is achieved by combining sampling with sequential approximations in such a manner as to reduce the computational effort in generating a new piecewise linear approximation in each iteration.

In 2-SD, a newly sampled outcome vector $\omega^k := (\omega_1^k, \ldots, \omega_N^k)$ is incorporated into a collection of existing outcomes, $\{\omega^1, \ldots, \omega^{k-1}\}$, at iteration $k$. The algorithm constructs a lower bounding linear approximation of the sample mean function

$$H_k(x) = \frac{1}{k} \sum_{j=1}^{k} h(x, \omega^j). \tag{3}$$

2-SD theory [14] suggests that asymptotic convergence can be achieved by solving just one second-stage LP (1b) in any iteration. Furthermore, previously obtained data [on the optimal dual solutions for (1b)]can be used to define a lower bounding approximation of $h(x, \omega^j)$, for $j < k$.

For the most recent outcome $\omega^k$ and first stage decision $x^k$, we evaluate the recourse function $h(x^k, \omega^k)$ by solving (1b) and obtain the dual optimum solution $\pi_k^k$. This dual vector is added to a set $V_{k-1}$ of previously discovered optimal dual vectors. In other words, we recursively update $V_k = V_{k-1} \cup \pi_k^k$. Linear programming duality ensures that for $\pi \in V_k$, $\pi^\top [r(\omega^j) - Tx] \leq h(x, \omega^j)$ $\forall x$. Thus, in iteration $k$, we identify a dual vector in $V_k$ that provides the best lower bounding approximation at $\{h(x^k, \omega^j)\}$, for $j < k$ that is

$$\pi_j^k \in \arg\max\{\pi^\top [r(\omega^j) - Tx^k] \mid \pi \in V_k\}. \tag{4}$$

Note that the calculations in (4) are carried out only for previous observations as $\pi_k^k$ will provide the best lower bound at $h(x^k, \omega^k)$. We use these dual vectors $\{\pi_j^k\}_{j \leq k}$ to generate a lower bounding function for the $k^{th}$ sample mean function

$$H_k(x) \geq \frac{1}{k} \sum_{j=1}^{k} (\pi_j^k)^\top [r(\omega^j) - Tx]. \tag{5}$$

Similar to Benders' decomposition, the lower bound (right-hand-side in (5)) is added as a new linear piece of the piecewise linear approximation of $\mathbb{E}\{h(x, \tilde{\omega})\}$.

One more distinction from deterministic decomposition is the periodic re-adjustment of previous linear pieces in 2-SD [14]. Note that in (5), with increasing iterations we use a larger number of samples to generate the linear approximation. Also, the linear piece at iteration $j < k$ lower bounds the sample mean $H_j(x)$ and not $H_k(x)$. As a result, the earlier linear pieces need to be re-adjusted to ensure that they continue to provide lower bounds on the current sample mean $H_k(x)$. If we assume, without loss of generality, that $h(x, \tilde{\omega}) \geq 0$ (almost surely), then we have $H_k(x) \geq j/k H_j(x) (j = 1, \ldots, k-1)$. Hence, the previously updated subgradient of the function $H_j$ can be used as a lower bounding function of $H_k$ by multiplying it by a factor of

$(j/k)$. With this, the approximation for the first-stage objective function at iteration $k$ is given by

$$f_k(x) := c^\top x + \max_{j=1,\ldots,k} \left\{ \frac{j}{k} \times \frac{1}{j} \sum_{i=1}^{j} (\pi_i^j)^\top [r(\omega^i) - Tx] \right\}. \quad (6)$$

Note that these approximations are generated in a recursive manner. The sequence $\{x^k\}$ is generated by 2-SD such that

$$x^{k+1} \in \arg\min\{ f_k(x) + \frac{1}{2}\|x - \bar{x}^k\|^2 \mid Ax \leq b\} \quad (7)$$

where $\bar{x}^k$ denotes an incumbent solution (the best solution) at iteration $k$ [14]. This incumbent is updated with the current solution ($\bar{x}^{k+1} = x^{k+1}$) if the (sample mean) point estimate of the objective value at $x^{k+1}$ is better than the estimate at $\bar{x}^k$; else, $\bar{x}^{k+1} = \bar{x}^k$.

Deterministic algorithms which solve convex programs by constructing an outer linearization of the objective function [20] are terminated when the difference between the objective function value at a given iterate and a valid lower bound on the objective function values is sufficiently small. The lower bounds obtained by 2-SD are based on sampled information, and hence are stochastic. Therefore, the deterministic termination criterion cannot directly be applied to a sampling based algorithm. The 2-SD approach uses a bootstrapping method to assess the primal-dual gap stability. The algorithm also gauges the impact of new information (new outcome $\omega^k$, new first stage candidate solution $x^k$, and new dual solutions $\pi_k^k$) on the approximation in (6). A measure of this impact and the primal-dual gap stability are used in designing the stopping rules for 2-SD. We refer the reader to [22] and [23] for details about these stopping rules.

The 2-SD algorithm has previously been applied to operations management [24], VLSI design optimization [25], chemical plant expansion [26], water resource engineering [27], among others. This work is the first application of 2-SD algorithm to the stochastic economic dispatch problem. The 2-SD algorithm offers several features which make it amenable for power systems applications:

- *Online sampling:* The 2-SD algorithm does not rely on a-priori selection of scenarios to be used for optimization. Rather, a new sample $\omega^k$ is introduced to the observation pool in every iteration, and the approximations are updated based on information collected at $(x^k, \omega^k)$. This allows updated forecast scenarios to be included without having to restart the optimization. As a result simulators are easily incorporated as a source of scenarios during optimization. Such simulators are currently used by system operators for diagnosis rather than optimization.
- *Computational edge:* Efficient implementation of (4) and (6), and use of the appropriate data structures [28] allow 2-SD to be used for large scale stochastic optimization problems, often encountered in power systems operations, using minimal computational resources.

## III. Computational Results

Our computational studies will address the main questions raised in the introductory section.

*1) Experiments:* For our computational study we consider the following experiments:

A) *Comparison of solution methods*. Here we will compare the 2-SD and ESF solution methods.
B) *Sensitivity to Dispatch Interval*. To study the effect of aggregation we solve both the systems with varying dispatch resolution using 2-SD at 10% wind integration level.
C) *Wind Penetration Study:* An increase in penetration level results in greater variability in renewable generation. We investigate the performance of 2-SD and the impact of model choice (hourly v sub-hourly) in systems with different renewable penetration levels.

Our experiments begin by first predicting an optimal or near optimal first stage solution for all instances. In the posterior analysis, the quality of these predicted first stage solutions is verified by fixing them and simulating the dispatch problem (1b) for different wind power realizations. This verification is terminated when a $(1-\alpha) \times 100\%$ confidence interval (CI) of total cost is built. In presenting the verification results we report the estimated mean and the 95% confidence interval of total cost.

*2) Experimental Setup: Test Systems:* The study was conducted on two energy networks, the IEEE-RTS96 1-Area system and the Illinois system. The RTS96 system [29], shown in Fig. 2(a), is an enhanced test system which has been used in several power system studies [5], [30]. This system is developed based on the data presented in [5], [29], and [30] and is modified to include a renewable generator and additional reserves. The system contains 32 thermal generators which produce electricity at generation costs which are functions of the fuel costs and average heat-rates. The load profile used is for a summer weekday. The spatial distribution of demand across the RTS96 system is derived based on Table II [29].

The second system [Fig. 2(b)] is based on realistic data available for the state of Illinois and comprises of 1900 buses, 2538 transmission lines, and 870 load nodes. The total system demand for the study horizon is 98 639.37 MWh. The system comprises of 237 internal generators and 24 intertie connections. The data consists of a detailed description of network topology, fuel costs, generator ramping constraints and capacities. Twelve wind farm locations at out-of-state buses are included in the network. For both these systems we assume that all the generators are committed over the horizon considered, and are available for dispatch. The demand is assumed to be constant over a 1-h time period.

*3) Wind Simulator:* The two-stage formulation in (1b), and the ESF formulation (2) allow for randomness in wind generation. The ESF models are built using the weather research and forecasting (WRF) outputs from [31] for 12 wind farm locations in Illinois. The WRF outputs are also used to build a vector autoregression based model. This model uses multiple WRF trial outputs to estimate its parameters, and allows for fast and efficient simulation of wind scenarios for use within stochastic programming algorithms. The model captures the spatio-temporal correlations of wind generation and uses a adaptive sliding window technique to overcome non-stationarity of high resolution, sub-hourly wind. We refer the reader to [32] for more details about the model. The 2-SD optimization and all verification runs for posterior analysis were carried out using scenarios simulated from this model.

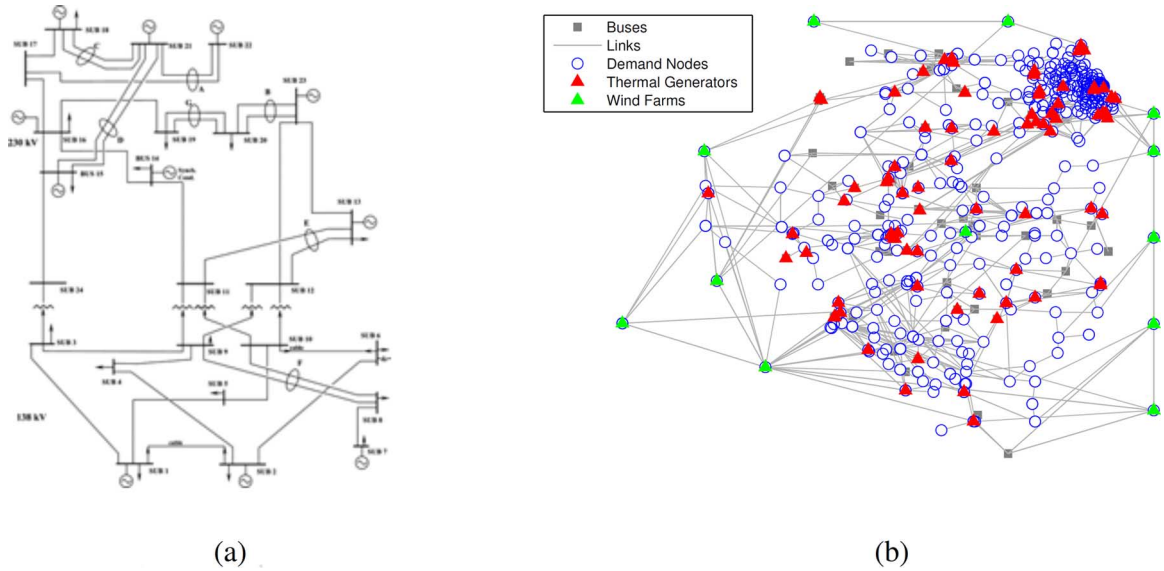


Fig. 2. Power systems under study. (a) RTS96 System. (b) Illinois System.

TABLE I
SOLUTION METHOD COMPARISON (10-MIN RESOLUTION, 10% WIND PENETRATION)

| System | Method | # scenarios | ESF Rows | ESF Columns | Predicted Value | Time (s) | Verification CI |
|---|---|---|---|---|---|---|---|
| RTS96 Hourly coupling | ESF | 10 | 11975 | 11552 | 40026.14 | 0.16 | [60074.26, 61697.02] |
| | | 20 | 23885 | 23072 | 40795.62 | 0.41 | [41385.75, 41443.03] |
| | | 30 | 35795 | 34592 | 40773.41 | 0.63 | [41385.06, 41442.35] |
| | | 100 | 119165 | 115232 | 40718.78 | 2.80 | [41385.04, 41442.33] |
| | 2-SD | 350 | - | - | 40945.71 | 2.35 | [40936.34, 40989.01] |
| Illinois Hourly coupling | ESF | 1(mean) | 40784 | 46337 | 18137161 | 128.83 | [22502915, 22620983] |
| | | 5 | 205538 | 234351 | 21886579 | 2866.56 | [22170843, 22272844] |
| | 2-SD | 181 | - | - | 22151783 | 768.67 | [22124133, 22213367] |
| Illinois Sub-hourly coupling | ESF | 1(mean) | 36415 | 40176 | 12878476 | 487.73 | [13737964, 13830823] |
| | | 5 | 179983 | 199836 | 12811076 | 4080.62 | [13722876, 13797483] |
| | 2-SD | 138 | - | - | 13721268 | 1147.28 | [13660228, 13742965] |

For the number of scenarios listed in Table I, the above data results in ESF formulations with sizes given by ESF Rows and ESF Columns in the table. Note that even for a small network such as RTS96, the size of the linear program easily grows to hundreds of thousands of rows and columns as the number of scenarios increase.

Although our computational experiments restrict the randomness $(\tilde{\omega})$ to wind power generation, the methodology is applicable to cases allowing randomness in demand, operating costs and generator outages.

*4) Platform:* The 2-SD algorithm was implemented in C programming language on a 64-bit Intel-core i7-2600 CPU @ 3.4GHzx8 with 8 GB of memory. All linear and quadratic programs were solved using CPLEX callable subroutines.

### A. Comparison of Solution Methods

For these experiments we use $t_H = 70$ min and $t_f = 60$ min for hourly coupling model. For the sub-hourly coupling instances $t_H$ is set to 60 min and $t_f$ is 10 min. Both the models allow variable generation data at $t_i = 10$-minute resolution.

The comparison results of 2-SD algorithm and limited sample ESF method are summarized in Table I. The predicted values reported refer to the objective function estimate of each optimization method (LP for ESF, and 2-SD). For 2-SD, one can interpret these values as estimates of lower bounds on the optimal value. The column labeled "Verification CI" (Confidence Interval) refers to the confidence interval calculated by simulating the consequences of first stage solution. These values correspond to estimates of the objective function at the first stage solution, and are therefore estimated upper bounds.

For sample-based stochastic programming models there is no guarantee that the predicted values for any instance will fall within the verification CI. This is observed in the case of ESF in Table I where the predicted values are lower than the verification CI for all sample sizes, indicating significant bias in predicting costs. Such bias arises due to the small sample sizes, and hence the quality of solutions from such small sample SP models is hard to discern. On the contrary, values predicted by the 2-SD algorithm use larger sample sizes, and hence have lower bias. This is emphasized by the fact that its prediction values fall within the verification CI which allows us to conclude that the solutions obtained are acceptable. Moreover, the verification column also shows that the estimated mean for 2-SD solutions are uniformly lower than the ones for ESF.

TABLE II
COMPARISON OF DISPATCH RESOLUTION (10% WIND PENETRATION)

| System | Resolution (min) | First stage resources (MWh) | Predicted value | Verification | | | |
|---|---|---|---|---|---|---|---|
| | | | | Mean | Std. Dev. | Confidence Interval | p-value |
| RTS Hourly coupling model | 10 | 2076.52 | 41409.59 | 41418.99 | 14.61 | [41390.35, 41447.64] | 1 |
| | 20 | 2076.96 | 41213.12 | 41423.42 | 14.61 | [41394.78, 41452.07] | 0.8303 |
| | 30 | 2074.08 | 41703.08 | 41765.22 | 31.70 | [41703.08, 41827.35] | $< 0.0001$ |
| | 60 | 2031.84 | 40449.79 | 55454.27 | 358.05 | [54843.49, 56247.04] | $< 0.0001$ |
| Illinois Hourly coupling model | 10 | 74258.8 | 29965989 | 29935161 | 30631 | [29875123, 29995200] | 1 |
| | 20 | 74035.9 | 29839346 | 29943153 | 31635 | [29881147, 30005160] | 0.8559 |
| | 30 | 73712.4 | 29741583 | 30027233 | 33473 | [29961624, 30092841] | 0.0425 |
| | 60 | 73340.3 | 29688063 | 30189580 | 40474 | [30110250, 30268909] | $< 0.0001$ |
| Illinois Sub-hourly coupling model | 10 | 74371.2 | 13721268 | 13701596 | 21106 | [13660228, 13742965] | 1 |
| | 20 | 74198.4 | 13596532 | 13726059 | 22744 | [13681480, 13770639] | 0.4302 |
| | 30 | 74069.4 | 13543494 | 13745003 | 23557 | [13702751, 13787255] | 0.1501 |
| | 60 | 74082.9 | 13522440 | 13907159 | 24177 | [13859771, 13954547] | $< 0.0001$ |

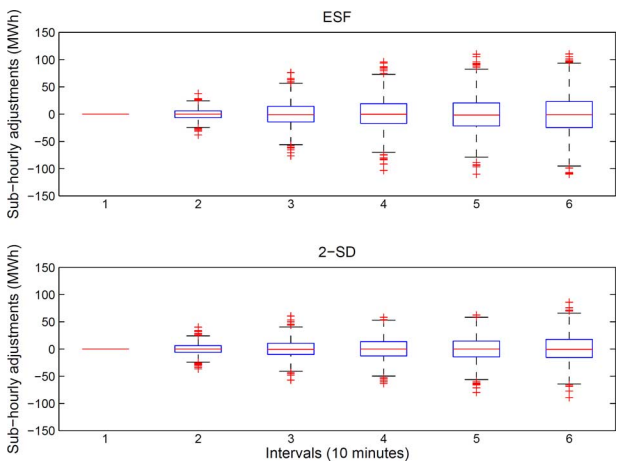


Fig. 3. Adjustments with sub-hourly coupling model in Illinois system.

Fig. 3 shows the adjustments of slow-response conventional generation in the sub-hourly coupling models. The recourse computed using a large set of scenarios allows 2-SD to predict solutions which require significantly lower adjustments at sub-hourly intervals when compared to the deterministic ESF approach, which is currently being used by operators. This is indicated by the fact that the adjustment intervals for 2-SD are completely enclosed within those for ESF (see Fig. 3).

Shifting our attention now to solution times for RTS96, note that as the number of scenarios increase for ESF, it loses its computational edge to 2-SD. This is, in fact, highlighted in the more realistic instance for the state of Illinois where ESF takes almost 50 min to manage 5 scenarios. On the other hand, 2-SD offers significant improvements in solution quality and computational times. This makes 2-SD an attractive method for solving large scale stochastic economic dispatch problems. Incidentally, the reader may find it interesting to note that if one were to use an ESF formulation to solve the Illinois instance using hourly coupling model reported in Table I, that linear program would have 7.2 million rows and 8.3 million columns.

As one can surmise, the predicted values obtained by 2-SD can also be significantly different from the verification CI. For such cases, we would expect to run the 2-SD algorithm with tighter stopping tolerance, so that the algorithm would use a larger number of samples, leading to improved gap estimates. However, this was not necessary for the instances encountered in this study.

### *B. Sensitivity to Dispatch Interval*

To account for hourly coupling constraints and varying resolutions ($t_i = 10, 20, 30,$ and 60 min) in hourly coupling model, a common $t_H = 120$ min is chosen for comparison in these experiments. In these instances slow-response generation and intertie decisions are held constant for a duration of $t_f = 60$ min. The sub-hourly coupling model uses $t_H$ of 60 min, over which only intertie decisions are held constant, while the slow-response generation decisions can be updated at $t_i = 10, 20, 30,$ and 60 min.

The two-stage stochastic programming instances at varying dispatch intervals are solved using 2-SD. The solutions obtained from these instances are verified using the same set of wind scenarios. The prediction and verification results for all the instances are summarized in Table II. These results indicate that finer resolution dispatch instances lead to lower costs for both hourly and sub-hourly coupling models. The coarser resolution models underestimate the realistic costs as indicated by the predicted values in Table II. This is because, optimization in these instances is carried out with mean ensembles.

Recall that the slow-response conventional generation levels are fixed for $t_f = 60$ min in the hourly coupling model, while the variable generation data is available at varying intervals ($t_i = 10, \ldots, 60$ min). As the interval is decreased, the fine timescale fluctuations in variable generation are clearly evident during optimization and hence, in this model the first stage reacts cautiously by using more slow-response conventional generation and intertie resources as indicated in Table II. The need to avoid infeasibilities due to lack of transmission capacity also contributes to this increase. In the sub-hourly coupling model, although the slow-response conventional generation decisions can be revised every $t_i$ in an adaptive manner, they are limited by their ramping capability. Hence, the first stage uses fine grain data and increases the first stage resources.

Table II also lists the p-value, computed from the verification data, associated with the null hypothesis: there is no difference

TABLE III
WIND PENETRATION RESULTS WITH HOURLY COUPLING MODEL (10-MIN RESOLUTION, 70-MIN HORIZON)

| System | Wind Penetration | Prediction | | | | Verification | | |
|---|---|---|---|---|---|---|---|---|
| | | Samples | First stage resources (MWh) | Value | Time (s) | Mean | Std. Dev. | Confidence Interval |
| RTS96 | 10 % | 350 | 2076 | 40945.71 | 2.35 | 40962.68 | 13.44 | [40936.34,40989.01] |
| | 20 % | 366 | 1970 | 40147.65 | 2.33 | 40168.25 | 24.61 | [40120.02, 40216.47] |
| | 30 % | 359 | 1901 | 39371.52 | 2.20 | 39513.22 | 117.76 | [39282.40, 39744.03] |
| Illinois | 10 % | 181 | 74090.5 | 22151783 | 768.47 | 22168750 | 22763 | [22124133, 22213367] |
| | 20 % | 189 | 70940.0 | 38409069 | 746.21 | 38446352 | 50641 | [38347094, 38545610] |
| | 30 % | 171 | 67905.5 | 59381611 | 912.74 | 59307934 | 98733 | [59114417,59501451] |

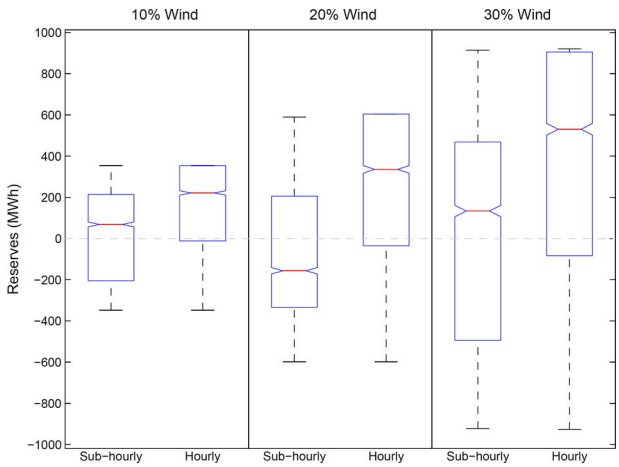


Fig. 4. Reserve utilization in Illinois System with Hourly Coupling Model.

between the 10-min dispatch solution and solution from lower resolution models. A p-value of less than 0.05, as seen for example in all 60-min dispatch instances, allows us to reject the null hypothesis at 95% significance level, and we can conclude that their solutions result in statistically different verification results. On the other hand, the null hypothesis cannot be rejected for 20-min dispatch instances, at 95% significance level.

Fig. 4 shows fast-response reserve utilization in Illinois system when hourly and sub-hourly (10-min interval) resolution is used with hourly coupling model. The positive and negative values indicate ramp up and down utilization respectively. Recall that this model uses committed reserve levels $(r_{ni}^{\min}, r_{ni}^{\max})$ as input, this is indicated by the outermost whiskers. The horizontal red lines with notches represent the median. The figure indicates that the reserve requirements increase with an increase in wind penetration levels. Further, the sub-hourly resolution models reduce reserve utilization for all penetration levels when compared to hourly resolution models.

### C. Wind Penetration Study

Thus far our computational experiments have demonstrated that both sample studies and coarse grain optimization have a potential to be misleading in their predictions (Table I, Table II). Such observations have also been made in simulations studies conducted by CAISO ([9], see I). Since 2-SD is a simulation-based optimization algorithm, we suspect that it should also be able to predict circumstances that cause congestion even when the dispatch is optimized. In this section we undertake a study to assess the performance of 2-SD at different wind penetration levels on both RTS96 and Illinois networks.

TABLE IV
ILLINOIS SYSTEM RESULTS WITH ADDED TRANSMISSION CAPACITY

| Wind% | Original | | Modified | |
|---|---|---|---|---|
| | Mean | Conv.gen.(MWh) | Mean | Conv.gen.(MWh) |
| 10 | 22168750 | 74090 | 9198967 | 70901 |
| 20 | 38446352 | 70940 | 7254406 | 62973 |
| 30 | 59307934 | 67905 | 5285322 | 54970 |

Energy penetration for this study is measured as the ratio of the amount of energy produced from the wind generation to the total energy produced. The results for 10%, 20%, and 30% wind integration for both the test networks are provided in Table III. These experiments were conducted on the hourly coupling model with $t_H = 70$ min, $t_f = 60$ min, and $t_i = 10$ min.

As expected, thermal generation is reduced as the availability of wind is increased. For the RTS96 system congestion was not encountered during 2-SD runs, and hence the net operational cost decreases when the penetration levels are increased (Table III). On the other hand, the initial experiments with the Illinois system identifies a small area of the network that needs congestion relief. In this area, increased penetration led to generation curtailment which in turn increased the overall operating cost of the system (Table III). Such identification of congestion is due to the combination of optimization and simulation within 2-SD.

Prompted by the specific areas of congestion we introduce additional capacity on a few links which alleviates such congestion. Table IV compares the verification results of the original Illinois system with the modified network. With additional transmission capacity the results indicate that the operational cost decreases with increased penetration. The reserve requirements also increase with the penetration levels due to increased volatility as shown in Fig. 4.

The 2-SD framework does not rely on a-priori sampling or knowledge of explicitly provided probability distribution. The algorithm learns the stochastic process in an online manner, and as a result, the number of samples necessary during the runs might vary (see Tables II and III). Table III also highlights the computational performance of 2-SD in instances with higher variability resulting from increased wind penetration. Moreover for congested networks, like the Illinois system at 30% penetration, a deterministic approach will choose a solution which can ensure feasibility only with respect to the sample(s) used to build the model. As a result, the system is much more prone to higher variability of reserves. On the other hand, 2-SD chooses first-stage solution which ensures feasibility across all the samples encountered during optimization. As before, the predicted

value falls within the verification confidence interval, and hence 2-SD provides good quality solutions even in the presence of high variability.

## IV. Conclusion

In this paper, we presented a stochastic economic dispatch framework which allows control of slow-response energy resources and intertie decisions at a coarse timescale, and renewable generation along with other dispatch related decisions at a fine timescale. To the best of our knowledge, this is the first study to incorporate sub-hourly economic dispatch within a stochastic optimization model. We presented two dispatch models which represent alternate operating practices used by power system operators. The results comparing these models at different resolutions illustrated the improvements that can be achieved by sub-hourly dispatch. The improvement in terms of the overall operational cost was due to effective utilization of sub-hourly information in deciding the first stage slow-response generation and intertie levels. The results at various wind integration levels showed reduction in operating reserve usage under sub-hourly dispatch. We also presented a stochastic programming approach, using 2-SD algorithm, to solve these large problems. The results demonstrated the scalability of 2-SD and showed that, when compared with extensive scenario formulation, 2-SD provided verifiably better solutions in far less time. Finally, the 2-SD algorithm was hooked with an external simulator which provided outputs for wind generation. Application of 2-SD algorithm over a rolling horizon, capturing economic dispatch over multiple hours, is currently being studied, and will be reported in the future. We will also investigate the role of storage devices in mitigating the challenges of renewable integration as part of our future research.

## Appendix
## Economic Dispatch Formulation

### A. Notation

We will use $n = 0$ to denote the first stage decision epoch. With $t_H$ denoting the model horizon and $t_i$ the sub-hourly interval, $N = t_H/t_i$ is the number of sub-hourly decision epochs. $\mathcal{N} = (1, \ldots, N)$ will denote these fine timescale decision epochs. The set of buses, links, demand and intertie nodes are denoted as $\mathcal{B}$, $\mathcal{L}$, $\mathcal{D}$, and $\mathcal{T}$, respectively. The set $\mathcal{G}$ constitutes the slow-response conventional generators, while the set of wind generators and fast-response reserves are denoted as $\mathcal{W}$ and $\mathcal{R}$, respectively. The subscript $i$ represents a subset of the respective set at bus-$i$.

The first stage variable $x$ consists of intertie decisions $T_i \forall i \in \mathcal{T}$ and slow response conventional generation levels $G_{0i} \forall i \in \mathcal{G}$. The corresponding production costs are denoted as $c_i^{tie}$ and $c_i^{gen}$, respectively.

Second stage variable $y$ includes ($\forall n \in \mathcal{N}$) the line-$(i,j)$ utilization $p_{nij}$ and bus-$i$ angle $\theta_{ni}$. Additional resources are available through committed fast-response reserves which are used to match energy imbalance resulting from stochastic realizations. These resources are limited by their availability, which is proportional to wind penetration, and is assumed to be known from prior unit/reserve commitment. These resources can provide both ramp-up and ramp-down capabilities and we will use $r_{ni}$ to denote utilization of these resources. Beyond this limit, the load can be curtailed by $r_{ni}^{ls}$ and the value of lost load is set at $d_i^{ls} \forall i \in \mathcal{L}$ (set to \$2000 in the computational study). Due to network constraints it is possible for generation at any particular node to be left unused. This generation can be ramped down only by a certain amount dictated by the physical ramping constraints. Generation beyond this limit is curtailed, which is denoted as $r_{ni}^{gs}$, and penalized by including a shedding penalty $d_i^{gs}$ at generation side ($\forall \mathcal{G}$). Finally, we treat wind generation as a must-take resource [33, Section III], provided there are sufficient reserves and no transmission issues in the system. To ensure this we impose a penalty $d_i^{ws}$ on wind curtailment $r_{ni}^{ws}$. These are also included as second stage decisions. For our computational study we have set these generation shedding penalty to \$500 (a value greater than the highest production cost). Alternately, market based settlement costs/opportunity costs can be used for these curtailment penalties.

The hourly coupling model also includes the intertie decisions and slow-response generation levels for next hour which are denoted as $T_i^+ \forall i \in \mathcal{T}$ and $G_{0i}^+ \forall i \in \mathcal{G}$, respectively. The inelastic load is denoted by $D_i$ for the current hour and $D_i^+$ for the next hour. The sub-hourly coupling model, on the other hand, has conventional generation revisions $G_{ni} \; \forall i \in \mathcal{G}$ and $\forall n \in \mathcal{N}$.

### B. Objective

For the hourly coupling model, the total cost comprises of the current intertie and conventional generation cost, and the expected value of recourse function. This recourse function includes the cost of generation for next hour and the penalty cost associated with wind, thermal and load curtailment:

$$\sum_{i\in\mathcal{T}} c_i^{tie} T_i + \sum_{i\in\mathcal{G}} c_i^{gen} G_{0i} + \mathbb{E}\Bigg\{ \sum_{i\in\mathcal{T}} c_i^{tie} T_i^+ + \sum_{i\in\mathcal{G}} c_i^{gen} G_{0i}^+ + \sum_{n\in\mathcal{N}} \Bigg( \sum_{i\in\mathcal{G}} d_i^{gs} r_{ni}^{gs} + \sum_{i\in\mathcal{D}} d_i^{ls} r_{ni}^{ls} + \sum_{i\in\mathcal{W}} d_i^{ws} r_{ni}^{ws} \Bigg) \Bigg\}. \quad (8)$$

For sub-hourly coupling model, the intertie and generation for next hour are not considered in the above function. However, the conventional generation revisions $G_{ni}$ are included at sub-hourly time intervals. For $n > 1$, the function is given by

$$\sum_{i\in\mathcal{T}} c_i^{tie} T_i + \frac{1}{N} \sum_{i\in\mathcal{G}} c_i^{gen} G_{0i} + \mathbb{E}\Bigg\{ \frac{1}{N} \sum_{i\in\mathcal{G}} c_i^{gen} G_{ni} + \sum_{n\in\mathcal{N}} \Bigg( \sum_{i\in\mathcal{G}} d_i^{gs} r_{ni}^{gs} + \sum_{i\in\mathcal{D}} d_i^{ls} r_{ni}^{ls} + \sum_{i\in\mathcal{W}} d_i^{ws} r_{ni}^{ws} \Bigg) \Bigg\}. \quad (9)$$

When $n = 1$, there are no sub-hourly revisions, and hence the term $G_{ni}$ is not included in (9). The objective is to minimize this cost subject to the constraints presented as follows.

### C. Hourly Constraints

These constraints are associated with slow-response generators.

a) *Generation capacity:*

$$G_i^{\min} \le G_{0i} \le G_i^{\max}, \quad (10)$$

$$G_i^{\min} \le G_{0i}^+ \le G_i^{\max} \quad \forall i \in \mathcal{G}. \quad (11)$$

$G_i^{\min}$ and $G_i^{\max}$ are the minimum and maximum generation capacity of generator units indexed by $i$.

b) *Ramping constraints:*

$$\Delta G_i^{\min} \leq G_{0i} - G_i^{init} \leq \Delta G_i^{\max}, \tag{12}$$

$$\Delta G_i^{\min} \leq G_i^{+} - G_{0i} \leq \Delta G_i^{\max} \quad \forall i \in \mathcal{G}. \tag{13}$$

$\Delta G_i^{\min}$ and $\Delta G_i^{\max}$ represent the down and up-ramping limits of generator units. Recall that the initial dispatch levels $\{G_i^{init}\}$ are known inputs to our models.

Constraints (10) and (12) appear as first stage constraints in (1a) for both the hourly and sub-hourly coupling models, while constraints (11) and (13) are bundled into second stage constraints (1b) only for the hourly coupling model. Note that these hourly constraints are not considered for aggregation.

### D. Sub-Hourly Constraints

The sub-hourly constraints are functions of both first and second stage variables. There will be one set of constraints, $\{\mathcal{F}(x, y_n, \omega_n)\}_{n\in\mathcal{N}}$, associated with each realization $\omega$ of the random variable $\tilde{\omega}$.

a) *Power flow equation*: If $n$ belongs to current hour

$$\sum_{j:(j,i)\in\mathcal{L}} p_{nji} - \sum_{j:(i,j)\in\mathcal{L}} p_{nij} - \sum_{j\in\mathcal{G}_i} r_{nj}^{gs} + \sum_{j\in\mathcal{R}_i} r_{nj} + \sum_{j\in\mathcal{W}_i} (\omega_{nj} - r_{nj}^{ws}) + \sum_{j\in\mathcal{G}_i} G_{0j} = \sum_{j\in\mathcal{D}_i} (D_j - r_{nj}^{ls}) \quad \forall i \in \mathcal{B}. \tag{14}$$

The power flow equations ensure that the supply meets the demand at every bus in the network. The next hour power flow equations for the hourly coupling model are obtained by replacing $G_{0j}$ with $G_{0j}^{+}$ and $D_j$ with $D_j^{+}$. Since sub-hourly coupling model allows for revision of conventional generation decisions at sub-hourly intervals, we will use $G_{nj}$ in the place of the static $G_{0j}$ in the above power flow equation.

b) *Line flow equation*:

$$p_{nij} = \frac{V_i V_j}{X_{ij}}(\theta_{ni} - \theta_{nj}) \quad \forall (i,j) \in \mathcal{L}, n \in \mathcal{N}. \tag{15}$$

Here $V_i$'s are the bus voltages and $X_{ij}$ is line reactance. The real power transmitted on any line and power loss on it are non-linear functions of the difference between the angles at the buses connected by the line. Second-order approximations are used to linearize these functions which make it suitable to be used with standard linear optimization methods. The power flow losses in the network are ignored in this formulation and only the line power flows are considered. [34] provides the details on this linearization of network constraints.

c) *Reserve limits*: Sub-hourly energy imbalance can be addressed using fast-response reserves which are limited by their availability:

$$r_{ni}^{\min} \leq r_{ni} \leq r_{ni}^{\max} \quad \forall i \in \mathcal{R}, n \in \mathcal{N}. \tag{16}$$

The limits $r_{ni}^{\min}$ and $r_{ni}^{\max}$ are available through reserve commitments, and are inputs to our models.

d) *Sub-hourly revisions*: The sub-hourly coupling model allows for sub-hourly revision of conventional generation which are limited by ramp rates of these generators. For $n = 0, \ldots, N-1$

$$\Delta G_i^{\min}(N) \leq G_{n+1i} - G_{ni} \leq \Delta G_i^{\max}(N), \forall i \in \mathcal{G}. \tag{17}$$

The ramping limits are dependent on $t_i$, and hence we denote them as functions of $N$.

e) *Bounds*: The bounds on the second stage variables are enforced due to the physical constraints on the network. $(p_{ij}^{\min}, p_{ij}^{\max})$ set the limits on the line capacities and $(\theta_i^{\min}, \theta_i^{\max})$ are the limits on the bus angles. The curtailment variables are limited by the amount of generation and load. For all $n \in \mathcal{N}$

$$p_{ij}^{\min} \leq p_{nij} \leq p_{ij}^{\max} \quad (i,j) \in \mathcal{L}, \tag{18a}$$

$$\theta_i^{\min} \leq \theta_{ni} \leq \theta_i^{\max} \quad i \in \mathcal{B}, \tag{18b}$$

$$0 \leq r_{ni}^{gs} \leq G_{ni} \quad i \in \mathcal{G}, \tag{18c}$$

$$0 \leq r_{ni}^{ls} \leq D_i \quad i \in \mathcal{D}, \tag{18d}$$

$$0 \leq r_{ni}^{ws} \leq \omega_{ni} \quad i \in \mathcal{W}. \tag{18e}$$

For the hourly coupling model, the upper bound in (18c) is replaced by $G_{0i}$ for all $n \in \mathcal{N}$.

## ACKNOWLEDGMENT

The authors would like to thank Prof. R. Sioshansi for important discussions on this topic. The authors also would like to thank the editor and the referees for their insightful and timely comments.

## REFERENCES

[1] J. Wang, M. Shahidehpour, and Z. Li, "Security-constrained unit commitment with volatile wind power generation," *IEEE Trans. Power Syst.*, vol. 23, no. 3, pp. 1319–1327, Aug. 2008.

[2] A. Papavasiliou, S. S. Oren, and B. Rountree, "Applying high performance computing to transmission-constrained stochastic unit commitment for renewable penetration," *IEEE Trans. Power Syst.*, accepted for publication.

[3] S. Ryan *et al.*, "Toward scalable, parallel progressive hedging for stochastic unit commitment," in *Proc. IEEE Power and Energy Soc. General Meeting*, 2013.

[4] R. Doherty and M. O'Malley, "A new approach to quantify reserve demand in systems with significant installed wind capacity," *IEEE Trans. Power Syst.*, vol. 20, no. 2, pp. 587–595, May 2005.

[5] J. Morales, A. Conejo, and J. Perez-Ruiz, "Economic valuation of reserves in power systems with high penetration of wind power," *IEEE Trans. Power Syst.*, vol. 24, no. 2, pp. 900–910, May 2009.

[6] Y. Makarov *et al.*, "Incorporating wind generation and load forecast uncertainties into power grid operations," in *PNNL-19189*, Jan. 2010.

[7] "Integration of variable energy resources," U.S. Federal Energy Regulation Commission, Order No. 764, 2012.

[8] "FERC order 764 compliance 15-minute scheduling and settlement," CAISO Rep., 2013.

[9] U. Helman *et al.*, "Integration of Renewable Resources: Operational Requirements and Assessment of Generation Fleet Capability at 20% RPS Requirement," CAISO Rep., 2010.

[10] E. Ela and M. O'Malley, "Studying the variability and uncertainty impacts of variable generation at multiple timescales," *IEEE Trans. Power Syst.*, vol. 27, no. 3, pp. 1324–1333, Aug. 2012.

[11] B. F. Hobbs and A. Hepenstal, "Is optimization optimistically biased?," *Water Resources Res.*, vol. 25, no. 2, pp. 152–160, 1989.

[12] J. Wang *et al.*, "Stochastic unit commitment with sub-hourly dispatch constraints," *Appl. Energy*, vol. 105, pp. 418–422, 2013.

[13] H. Heitsch and W. Romisch, "Scenario reduction algorithms in stochastic programming," *Computat. Optimiz. Applicat.*, vol. 24, no. 2-3, pp. 187–206, 2003.

[14] J. L. Higle and S. Sen, "Finite master programs in regularized stochastic decomposition," *Math. Program.*, vol. 67, no. 1-3, pp. 143–168, 1994.
[15] A. Papavasiliou, S. Oren, and R. O'Neill, "Reserve requirements for wind power integration: a scenario-based stochastic programming framework," *IEEE Trans. Power Syst.*, vol. 26, no. 4, pp. 2197–2206, Nov. 2011.
[16] C. Zhao and Y. Guan, "Unified stochastic and robust unit commitment," *IEEE Trans. Power Syst.*, vol. 28, no. 3, pp. 3353–3361, Aug. 2013.
[17] Y. Dvorkin *et al.*, "A hybrid stochastic/interval approach to transmission-constrained unit commitment," *IEEE Trans. Power Syst.*, to be published.
[18] S. Sen, "Stochastic programming," in *Encyclopedia of Operations Research and Management Science*, S. Gass and M. Fu, Eds. New York, NY, USA: Springer, 2013, pp. 1486–1497.
[19] E. Erik, M. Milligan, and B. Kirby, "Operating Reserves and Variable Generation," NREL Tech. Rep., 2011.
[20] J. Benders, "Partitioning procedures for solving mixed-variables programming problems," *Numer. Math.*, vol. 4, no. 1, pp. 238–252, 1962.
[21] R. M. V. Slyke and R. Wets, "L-shaped linear programs with applications to optimal control and stochastic programming," *SIAM J. Appl. Math.*, vol. 17, no. 4, pp. 638–663, 1969.
[22] J. L. Higle and S. Sen, "Statistical approximations for stochastic linear programming problems," *Ann. Oper. Res.*, vol. 85, no. 0, pp. 173–193, 1999.
[23] S. Sen and Y. Liu, "Technical Mitigating Uncertainty via Compromise Decisions in Two-Stage Stochastic Linear Programming," Data Driven Decisions Lab, Univ. Southern California, 2014.
[24] P. Mirchandani and A. K. Mishra, "Component commondality: models with product-specific service constraints," *Prod. Oper. Manage.*, vol. 11, no. 2, pp. 199–215, 2002.
[25] V. Khandelwal and A. Srivastava, "Monte-Carlo driven stochastic optimization framework for handling fabrication variability," in *Proc. IEEE/ACM Int. Conf. Comput.-Aided Design (ICCAD)*, Nov. 2007, pp. 105–110.
[26] S. Frausto-Hernandez, V. Rico-Ramirez, and I. E. Grossmann, "Strategic capacity allocation under uncertainty by using a two-stage stochastic decomposition algorithm with incumbent solutions," *Ind. Eng. Chem. Res.*, vol. 49, no. 6, pp. 2812–2821, 2010.
[27] D. Zhang, Z. Lu, and G. Liu, "An efficient stochastic decomposition approach for large-scale subsurface flow problems," in *Proc. XVI Computational Methods for Water Resources*, 2006.
[28] J. L. Higle and S. Sen, *Stochastic Decomposition: A Statistical Method for Large Scale Stochastic Linear Programming*. Boston, MA, USA: Kluwer, 1996.
[29] C. Grigg *et al.*, "The IEEE reliability test system-1996. a report prepared by the reliability test system task force of the application of probability methods subcommittee," *IEEE Trans. Power Syst.*, vol. 14, no. 3, pp. 1010–1020, Aug. 1999.
[30] F. Bouffard, F. Galiana, and A. Conejo, "Market-clearing with stochastic security-part II: case studies," *IEEE Trans. Power Syst.*, vol. 20, no. 4, pp. 1827–1835, Nov. 2005.
[31] V. Zavala *et al.*, "Computational and economic limitations of dispatch operations in the next-generation power grid," in *Proc. IEEE Conf. Innovative Technologies for an Efficient and Reliable Electricity Supply (CITRES)*, 2010, pp. 401–406.
[32] H. Gangammanavar, "Multiple timescale stochastic optimization with application to integrating renewable resources in power systems," Ph.D. dissertation, Ohio State Univ., Columbus, OH, USA, 2013.
[33] L. Bird, J. Cochran, and X. Wang, "Wind and Solar Energy Curtailment: Experience and Practices in the United States," NREL Tech. Rep., 2014.
[34] A. Motto *et al.*, "Network-constrained multiperiod auction for a pool-based electricity market," *IEEE Trans. Power Syst.*, vol. 17, no. 3, pp. 646–653, Aug. 2002.

**Harsha Gangammanavar** received the M.S. degree in electrical engineering and the Ph.D. degree in operations research from the Ohio State University, Columbus, OH, USA, in 2009 and 2013, respectively.

He is currently a Visiting Assistant Professor at the Daniel J. Epstein Department of Industrial and Systems Engineering at the University of Southern California, Los Angeles, CA, USA.. His research interests are focused on stochastic programming and approximate dynamic programming for energy systems operations and planning.

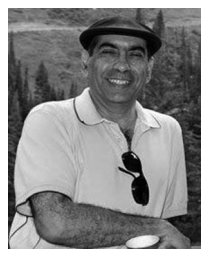

**Suvrajeet Sen** is a Professor at the Daniel J. Epstein Department of Industrial and Systems Engineering at the University of Southern California, Los Angeles, CA, USA. Until recently (2012), he was a Professor of Integrated Systems Engineering at the Ohio State University, where he also served as the Director of the Center for Energy, Sustainability and the Environment, and led the Data Driven Decisions Lab. Over the years, he has held several other positions, including Professor at the University of Arizona, and a Program Director of Operations Research, as well as Service Enterprise Systems at the National Science Foundation (NSF).

Prof. Sen is a Fellow of INFORMS. He has served on several editorial boards, including *Operations Research* as Area Editor for Optimization and as Associate Editor for *INFORMS Journal on Computing*, *Journal of Telecommunications Systems*, and *Operations Research*. He also serves as an Advisory Editor for several newer journals. He was also instrumental in founding the INFORMS Optimization Section in 1995, and is currently serving as Chair of the INFORMS Optimization Society.

**Victor M. Zavala** received the B.Sc. degree from Universidad Iberoamericana, Mexico City, Mexico, in 2003 and the Ph.D. degree from Carnegie Mellon University, Pittsburgh, PA, USA, in 2008, both in chemical engineering.

He is currently a computational mathematician in the Mathematics and Computer Science Division at Argonne National Laboratory, Argonne, IL, USA, and a Fellow in the Computation Institute of the University of Chicago, Chicago, IL, USA. His research interests are in the areas of mathematical modeling and large-scale optimization of infrastructure systems.